INSTITUTE OF PHYSICS PUBLISHING CLASSICAL AND QUANTUM GRAVITY

Class. Quantum Grav. **22** (2005) S287–S296 doi:10.1088/0264-9381/22/10/021

Advanced gravitational reference sensor for high precision space interferometers

Ke-Xun Sun, Graham Allen, Sasha Buchman, Dan DeBra and Robert Byer

Hanson Experimental Physics Laboratory, Stanford University, Stanford, CA 94305-4085, USA

E-mail: kxsun@stanford.edu

Received 8 November 2004, in final form 18 January 2005
Published 26 April 2005
Online at stacks.iop.org/CQG/22/S287

Abstract

LISA and the next generation of space-based laser interferometers require gravitational reference sensors (GRS) to provide distance measurements to picometre precision for LISA, and femtometre precision for the proposed Big Bang Observatory (BBO). We describe a stand-alone GRS structure that has the benefits of higher sensitivity and ease of fabrication. The proposed GRS structure enables high precision interferometric links in three-dimensional directions. The GRS housing provides the optical reference surface onto which the transmitted laser beam, and the independent received laser beam are referenced. The stand-alone GRS allows balanced optical probing of the distance of the proof mass relative to the housing at a power and wavelength that differ from the transmitted and received wavelengths and with picometre sensitivity without radiation pressure imbalance. The single parameter that reduces proof mass disturbance forces is the gap spacing. Optical readout allows the use of a large gap between the GRS housing and proof mass. We propose using rf-modulated optical interferometry to measure both relative displacement and absolute distance. Further we propose to use a reflective grating beamsplitter within the GRS and on the external optical bench. The reflective grating design eliminates the in-path transmissive optical components and the dn/dT related optical path effects, and simplifies the optical bench structure. Inside the GRS, a near-Littrow mounted grating enables picometre precision measurement at microwatts of optical power. Preliminary experimental results using a grating beamsplitter interferometer are presented, which demonstrate an optical sensing sensitivity of 30 pm $Hz^{-1/2}$.

PACS numbers: 04.80.Nn, 95.55.Ym, 07.60.Ly, 42.79.Dj, 42.40.Eq, 42.79.−f

1. Introduction

The gravitational reference sensor (GRS) provides an inertial reference in spacetime to enable time varying position and distance measurement. The GRS is the central element of a drag-free inertial system. The drag-free inertial system, called the disturbance reduction system (DRS), is comprised of the GRS, a feedback control system that positions the satellite precisely around the inertial proof mass, and the micro-thrusters that are controlled to position the satellite.

The GRS technology is currently being developed for several space missions including gravitational wave astronomy, for example, ST-7/LISA Pathfinder (LTP) and LISA [1–3], as well as other fields, such as satellite tests of the equivalence principle and terrestrial gravity field mapping. LISA and the GRACE follow-on missions require that the GRS provide a precision measurement to the proof mass of 5–20 pm $\text{Hz}^{-1/2}$ in the frequency range from 0.1 mHz to 1 Hz. The Big Bang Observatory (BBO) [4], the LISA follow-on mission, will require a measurement precision of $\sim$1 fm $\text{Hz}^{-1/2}$ from 0.1 to 10 Hz.

An important aspect of technology development is to explore further improvements of the GRS configurations to reduce complexity and to enhance the measurement precision. Here we describe an advanced GRS structure that will be more sensitive to the science signal, less susceptible to noise, simpler to implement and perhaps less costly to engineer.

2. The stand-alone GRS

In the current GRS design for LISA, the laser beam received from the remote spacecraft is transmitted through a series of optics to illuminate the proof mass first and then is reflected back and onto the optoelectronic detector where it interferes with the laser local oscillator reference. The proof mass acts as the gravitational reference surface. However, the local laser that produces the optical phase reference is fixed on the bench attached to the spacecraft. Therefore, the detected signal contains the phase noise induced by spacecraft motion even though the sensitive path involves a trip to proof mass. The error signal due to relative motion can be cancelled by detection of the relative motion between the back surface of the proof mass and the spacecraft. This complexity can be avoided by directing the received laser beam to the detector without illuminating the proof mass, while having separate internal measurements.

To date, capacitive sensing has been explored as the positional measurement technique to measure the GRS proof mass location relative to the housing that surrounds the proof mass. For example, in both GP-B and ST-7, capacitive sensing is used. One of the intrinsic difficulties in capacitive sensing is that increasing the measurement sensitivity also raises the disturbance forces. To enhance the sensitivity, the capacitive sensing requires higher driving voltage and smaller gaps. However, the by-product is increased back action to the proof mass, thus increased residual acceleration and sensitivity to external forces. A minimum displacement sensitivity of 1–3 nm $\text{Hz}^{-1/2}$ for capacitive sensing is the sensing limitation for both the LISA Pathfinder Package (LTP) and ST7. Optical readout can reach the picometre or higher sensitivity requirements without exerting excessive back action. The future development of advanced drag-free formation flying satellite missions necessitates optical readout to be included in the GRS sensing technology.

Based on these considerations, we propose a stand-alone GRS structure, which has the benefits of both higher sensitivity and ease of fabrication. The proposed GRS structure enables high precision interferometric links in three-dimensional directions. The GRS housing provides the optical reference surface onto which the transmitted and the received laser beams are referenced. The stand-alone GRS incorporates balanced, low-power optical measurements to picometre sensitivity within the GRS housing, and allows the freedom to optimize the laser

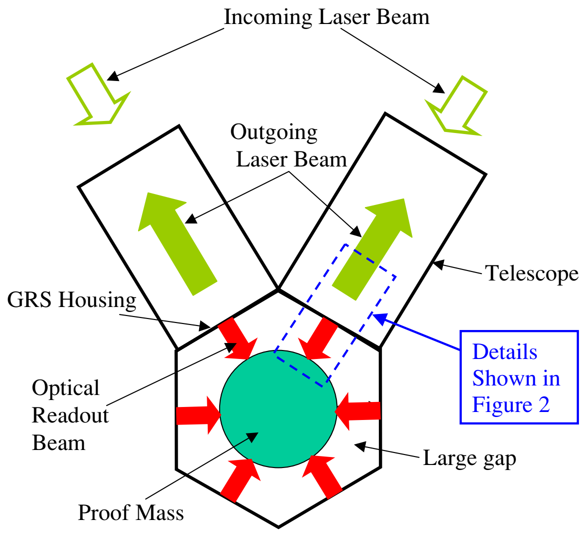

Figure 1. The concept of the advanced GRS in the form appropriate for the LISA mission with two telescopes. The transmit/receive laser sources and detectors are separate from the optical readout sources and detectors. This requires that the centre-of-mass location be transferred from inside the GRS housing to a reference surface on the outside of the GRS housing with picometre precision. The means for accomplishing this are illustrated in figure 2.

transmitted power and wavelength for sub-optical wavelength precision measurement to distant satellites [5].

The stand-alone GRS also reduces complexity by merging the two cubic proof masses, proposed for the LISA mission, into one spherical mass. This eliminates the costly and complex back surface fibre coupling from one proof mass to the other, and with it the inter-proof-mass noise. With proper algorithms, the stand-alone GRS, with a single proof mass design, permits determination of the centre of mass of the proof mass with minimum disturbance. The stand-alone GRS with optical sensing enables a true drag-free approach in which the proof mass operates with zero stiffness. It becomes an anchor to inertial spacetime.

Figure 1 shows the key features of the proposed stand-alone GRS configuration. The stand-alone or modularized GRS approach is well suited to a variety of space missions because it can be adapted to meet sensitivity and configuration requirements. The GRS utilizes a double-sided grating element in the wall of the GRS housing to transfer the GRS centre-of-mass position information from inside the GRS housing to the external reference surface outside the GRS housing with picometre precision. The GRS uses optical readout of the gap distance between the housing and the proof mass. The single parameter that reduces the disturbance of the proof mass is the gap spacing. Optical readout allows the use of a large gap between the GRS housing and the proof mass. The precision of the optical readout is picometre or higher. The advanced GRS uses all-reflective grating beamsplitters for both the GRS internal gap distance interferometer and the external laser interferometer. The all-reflective interferometer design eliminates in-path transmissive optical components (windows) and their $\mathrm{d}n/\mathrm{d}T$ optical path variations with temperature. The GRS uses optical fibres to deliver and receive optical radiation to and from, but not within, the critical interferometer paths. This eliminates the need for an optical bench structure, reduces weight and size, and allows key optical components such as detectors and laser sources to be located remotely from the sensitive GRS unit. The GRS utilizes multiple optical sensors to measure the centre-of-mass position and movement of the proof mass with accuracy and redundancy. The measurement is robust against environmental changes such as temperature variation, mechanical disturbance and mechanical deformations of the GRS housing. The grating interferometer allows correction for point ahead and tracking angles to distant satellites by proper grating design and by moving small secondary and tertiary mirrors in the telescope similar to the Webb Telescope approach, thus avoiding mass movements on the spacecraft.

Of historic interest, the idea of combining the two cubic proof masses appeared in an earlier LISA study [1]. The external laser beams stopped at the housing surface as here. However, due to the faceted proof mass shape, proof mass orientation must be controlled by forcing and, in this sense, the LISA study concept is one step away from a true drag-free GRS.

3. Optical sensing versus capacitive sensing

Before delving into further details of our proposed GRS structure, we present a brief but quantitative discussion of the advantages of optical sensing over capacitive sensing: higher sensitivity and very low back action.

The practical readout sensitivity of the optical sensing is limited by shot noise in optoelectronic detection. For a typical wide-band interferometer, the shot noise limited length measurement sensitivity is given by

$$\Delta l \approx \frac{1}{\pi}\left(\frac{hc\lambda}{2\eta P}\right)^{1/2} \tag{1}$$

where P is the laser power, c is the speed of light, h is the Planck constant, λ is the laser wavelength and η is the detector quantum efficiency. At 1.5 μm wavelength, the optical power needed to reach picometre precision is less than 1 μW, which is very low and thus insufficient power to lead to heating.

The back action generated by the radiation pressure induced by the optical beam is determined by the momentum transfer from laser beam to the proof mass. The back action force along the input beam direction is bounded by

$$F_{\text{optical}} = \frac{P}{c}\left(1 + \iint R(\theta,\varphi)\cos(\theta)\,\mathrm{d}\Omega\right) < \frac{2P}{c}, \tag{2}$$

where $R(\theta, \varphi)$ is the proof mass surface power reflectivity with angular dependence. At 1 μW, which allows a sub-picometre measurement precision, the total force is 6.67×10^{-15} N. For a proof mass of 2 kg, the deterministic acceleration is 3.3×10^{-15} m s^{-2}. An opposite optical beam with imbalance less than 1%, which is easily feasible, will reduce the static acceleration to 3.3×10^{-17} m s^{-2}, well below the LISA requirement. The optical readout can be considered as stiffness-free, effectively decoupling the spacecraft motion from the proof mass.

4. All-reflective optical readout based on diffractive optics

An important feature in our proposed advanced GRS is the all-reflective diffractive optics based sensing. In an all-reflective optics arrangement, light in the interference region is not transmitted through the optics substrate or optical window. For a laser beam of wavelength λ incident onto the grating, the output angle θ_m of the mth diffraction order is given by the grating equation,

$$d(\sin\theta_m - \sin\theta_{\text{inc}}) = m\lambda, \tag{3}$$

where θ_{inc} is the incident angle and d is the grating period. An interferometer is formed when diffractive orders are overlapped and interfere.

The all-reflective, grating-based interferometer was originally investigated at Stanford University for high precision measurement for ground-based gravitational wave detection in 1996 [6]. The intention was to overcome thermal lensing in LIGO. All-reflective Michelson, Sagnac and Fabry–Perot interferometers based on grating beam splitters were demonstrated.

Similar but more fundamental thermal problems exist in high-precision space-based interferometers for gravitational wave detection. Temperature changes induce thermal expansion and refractive index changes ($\mathrm{d}n/\mathrm{d}T$) in the optical path length of any optical material. Thermally induced optical path changes lead to noise that may be confused with real gravitational wave signals. For example, the refractive index change for typical optical materials is about $10^{-5}\ \mathrm{K}^{-1}$, and is higher for optically dense materials such as waveplates. This requires a temperature stability of sub-micro-kelvin in the sensing band to reach optical path length stabilities of 1 picometre. All-reflective optics have zero optical path within the material and do not have a $\mathrm{d}n/\mathrm{d}T$ optical path length change. For many optical materials, optical path variation due to refractive index change induced by temperature is ten times larger than that due to thermal expansion. Therefore, reflective optics have better stability against temperature fluctuations.

For follow-on missions of LISA such as BBO, where higher laser power up to several hundreds watts is needed, the $\mathrm{d}n/\mathrm{d}T$ effect is more pronounced due to laser heating. Dielectric gratings, originally developed for use in laser fusion experiments [7, 8], are suitable for the advanced GRS applications. All-reflective grating beamsplitters use polarization selectivity but avoid large birefringence changes with temperature. All-reflective optical elements do not have mechanical-stress-induced birefringence. A transparent window on the proof-mass housing chamber can produce optical path variations due to differential stress caused by mounting the element.

There is a need to avoid, at all costs, the transmission of the interfering optical beams through optical components or windows. This suggests an all-reflective optical interferometer but leaves open the issue of transferring, with picometre precision, the centre-of-mass measurement within the GRS housing to a reference surface outside the GRS housing.

5. Internal and external interferometer structure with double-sided grating

The double-sided grating beamsplitter is the central component of the all-reflective interferometer for application to the advanced GRS. Figure 2 shows the details of the proposed advanced GRS structure that uses grating beamsplitters to form interferometers. One interferometer lies within the GRS housing and measures the gap with picometre precision. The second interferometer lies external to the GRS housing and is used to measure the distance to the remote spacecraft with the sub-wavelength precision limited by shot noise of the laser beam. The key is that the location of the GRS centre-of-mass position is referenced to the external reference surface through the back-to-back grating element that is part of the GRS housing wall. There are no windows and the external laser source is independent of the optical source used to illuminate the GRS proof mass.

Figure 2 shows the schematic of the stand-alone GRS wall section, and illustrates the thin two-sided grating that is the Littrow grating interferometer within the GRS and reference surface external to the GRS. This element transfers, with picometre precision, the centre-of-mass location to the external reference surface for the external laser interferometer. Further, it allows the two sides to be designed for different laser wavelengths. The inner side of the grating might be designed for an optical readout wavelength of 1500 nm. The outer

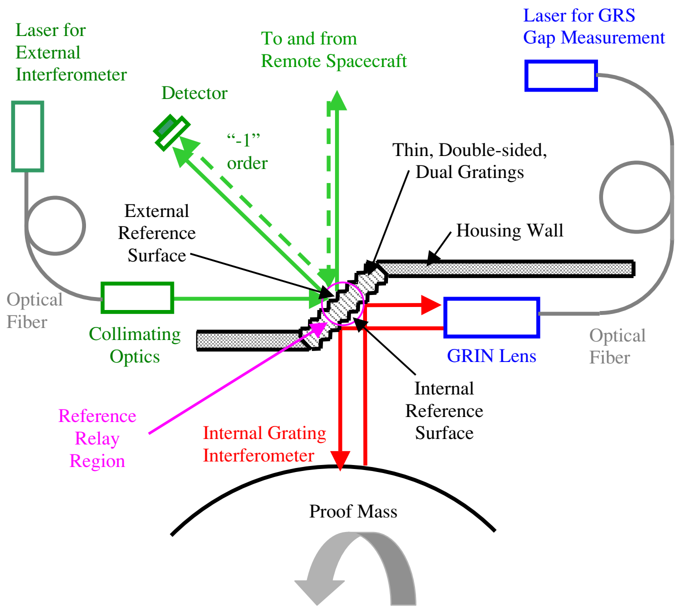

Figure 2. The detailed structure of the GRS internal optical sensor and external laser interferometer is illustrated. A double-sided grating is used to form both the internal GRS interferometer between the GRS wall and the proof mass, and the external interferometer that references the received laser beam to the local oscillator. The internal picometre precision measurement is relayed to the external interferometer at the reference relay region where laser beams from two sides are incident onto the back-to-back grating that is an element of the GRS housing wall.

side of the grating might be designed for the external laser interferometer with operation at 1064 nm or 532 nm wavelengths. What is key is that this element can be designed from a well-characterized material, silicon or fused silica, for example, with a very well-known thermal expansion coefficient so that its thickness is known versus temperature to picometre precision. The common reference element eliminates the need for a sizeable optical bench and majority of optical components. The parasitic optical path change is thus reduced by the compactness of the advanced GRS configuration. The thin gratings provide vacuum seal and are permanent elements incorporated into the stand-alone GRS housing.

As an example, the thickness of the double-sided grating can be taken as 2 mm. Assuming a thermal expansion coefficient of 0.4×10^{-6}, then the thermal expansion for 1 μK temperature change is 0.8 fm. When temperature variation reaches 1 mK or above, the thermal expansion can reach 1 pm. However, a temperature change of 1 mK can be accurately measured, and thermal expansion changes can be calibrated. In contrast, a group of transmissive optics that is designed to accomplish a similar GRS function would typically have a much larger $\mathrm{d}n/\mathrm{d}T$ induced optical path length change. Recent estimates are that at 1 μK temperature change, the optical path variation could reach 40 pm [9].

Also shown in figure 2 is the fibre optic for delivering and detecting the optical radiation to and from the interferometers. The upper portion shows the external laser interferometer, where the external reference laser path utilizes the grating on the outside of the GRS housing. The lower portion shows the GRS internal optical readout via a Littrow grating interferometer. The optical fibres allow the sources and the detectors to be placed remotely from the GRS unit, thus removing thermal disturbances from the region of the GRS. The optical fibres are

NOT part of the sensitive interferometer optical paths and thus do not introduce noise into the precision interferometer measurement. The use of optical fibre eliminates the need for macroscopic transmissive optical elements mounted onto a low expansion optical bench, thus reducing weight and cost.

6. Internal precision interferometry using Littrow grating cavity

In the first-order Littrow grating, the $m = -1$ diffraction order is back diffracted and overlapped with the incoming beam. The grating in this case forms a cavity input mirror with the power reflectance being the diffraction efficiency η in the -1 order. The proof mass surface acts as the end mirror. This Littrow resonator configuration is well known in the laser field where it has been used as a tunable laser cavity for dye lasers. When the cavity length varies, the resonated beam in the cavity varies in both amplitude and phase as with any Fabry–Perot interferometer. The fringes from the Littrow mounted grating cavity are similar to those observed in 1996 for the LIGO experiment [6], but with fibre optic transport. The optical fibres are *not* in the interferometer path, they simply transport light to and from the interferometer.

Multiple optical readout beams, for example a total of 18 beams, could be used in the advanced GRS. Symmetrical measurements are capable of measuring both the geometric and mass centres of the proof mass and the thermal expansion of the proof mass or the housing. Therefore, the proposed stand-alone GRS is more robust for a variety of space missions that may not have a stable temperature environment.

7. External precision GRS laser interferometry

The outer side of the double-sided grating is designed to be highly polarization sensitive. As shown in the example in figure 2, the external laser beam (solid green coloured in drawing) with its polarization lying in the plane of the laser beam and the grating normal will diffract into the zeroth order and be transmitted to remote spacecraft. The minor orthogonal polarization component will diffract onto the detector at the local oscillator. The incoming beam from the remote spacecraft is polarized orthogonal to the outgoing beam. By the property of scattering matrix, the incoming beam mostly diffracted onto the detector to mix with the local oscillator to produce the interference signal for the science measurement.

In a grating-based, stand-alone GRS, the external laser light does not illuminate the proof mass. Therefore, the high power external laser beam can be selected to optimize the measurement precision to the far spacecraft in both power and wavelength. For example, for LISA a green laser beam would improve the sensitivity. For BBO the extreme sensitivity would be met by using ultraviolet wavelengths such as the fourth harmonic of the Nd:YAG laser at 266 nm.

This configuration essentially has all the functions of the current LISA design but has a significantly simplified structure. Importantly, we have shown that by proper selection of the grating period, the incoming and outgoing beams can have a separation equal to the 'look ahead angle'. In the current design for LISA, the 'look ahead angle' is achieved by tilting the proof mass that, in turn, couples noise into the sensitive measurement axis.

8. Preliminary experiments on an all-reflective, grating interferometer

Recently we have conducted a preliminary, proof-of-principle experiment of the all-reflecting grating interferometer with fibre optics coupling. Figure 3 shows the experimental setup.

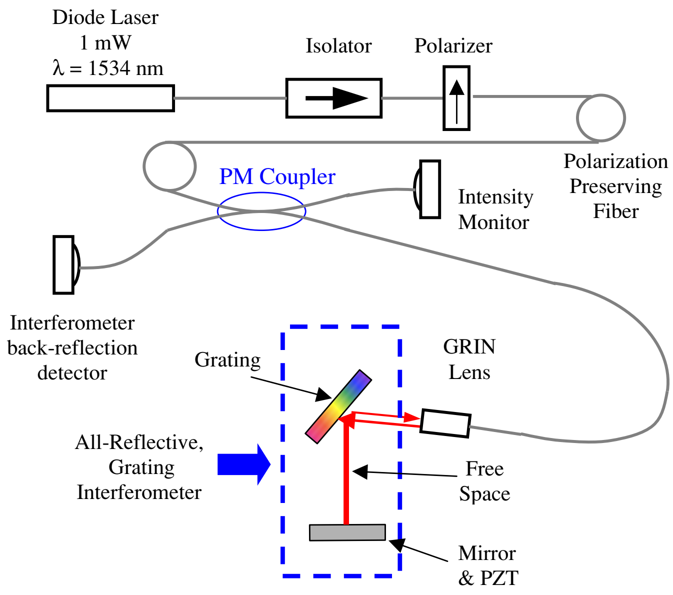

Figure 3. The experimental setup for laboratory test of the all-reflective grating interferometer. The laser radiation is transmitted to and from the grating interferometer through single-mode, polarization-preserving fibre.

As described in the previous sections, we used optical fibre as laser transport. We selected the cavity length to be 1.5 cm, similar to the expected GRS gap spacing. The light source is a wavelength stabilized laser diode providing 1.0 mW at 1534 nm. The GRIN lens is $\sim$5 mm from the grating and has an output beam waist $\sim$0.5 mm. The grating and the PZT-driven end mirror form the all-reflective interferometer. The grating has a line density of 830 lines/mm, giving a Littrow angle 39.5°. The all-reflective grating interferometer cavity is scanned using a PZT mounted on the end mirror. The GRIN lens provides collimated light to the grating interferometer. The grating and the end mirror form a Fabry–Perot cavity. The reflected light from the cavity is coupled back into the fibre by the GRIN lens, and serves as the position readout. The measurement is purely that of the separation of the proof mass surface from the GRS housing wall. Therefore, no noise is introduced into the picometre precision measurement by the use of the optical fibre for transport.

Figure 4 shows the reflected signal from the grating cavity when the end mirror position is scanned by a PZT. The effective voltage range for the periodic fringe is $\sim$900 mV. The corresponding displacement of the cavity mirror is a quarter wavelength, or 384 nm. The direct electronics readout precision in one scan is estimated to be at least $\sim$10 mV or 4.3 nm at this scan speed. The time interval for 10 mV signal variation at 50% Lorentzian dip is approximately 5 μs. The readout sensitivity, estimated crudely but conservatively, is thus $4300 \times \sqrt{5 \times 10^{-6}} \approx 10$ pm Hz$^{-1/2}$ around the fringe scan frequency. For a more 95% confidence claim, the readout sensitivity is $\sim$30 pm Hz$^{-1/2}$. The fringe scan frequency is approximately 800 Hz. Improved detection should extend the sensitivity to the LISA frequency band. Further measurement using a spectrum analyser will help with readout precision thanks to longer true integration time.

In this preliminary experiment, we only used a general purpose DFB semiconductor laser. The detection scheme was direct detection with direct amplification rather than heterodyne

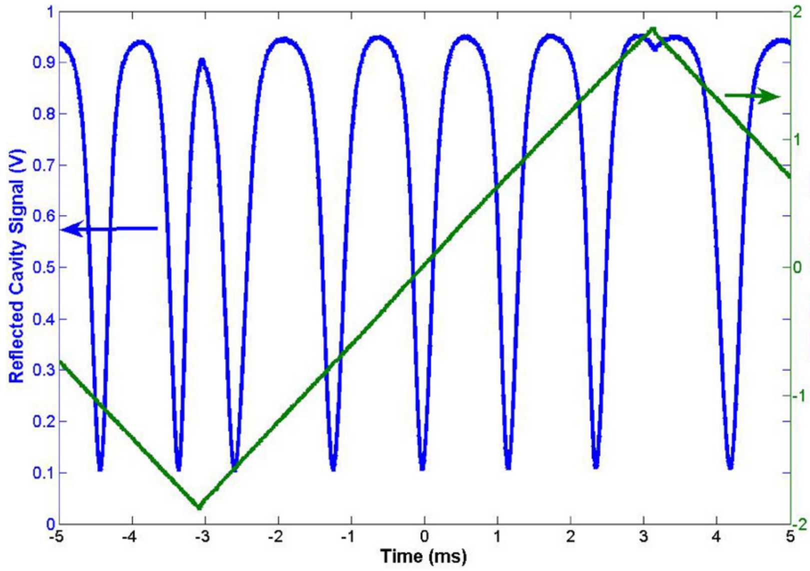

Figure 4. Measured optical fringes from the all-reflective grating interferometer. The sensitivity is determined to be $\sim$30 pm $\text{Hz}^{-1/2}$ in this preliminary experiment.

detection with rf amplification. The experiment was performed at higher power due to the lack of optimized detectors. We are planning improvements such as laser source stabilization, rf-heterodyne detection, synchronized demodulation and high-efficiency detection using small-area detectors. These measures should lower the laser power and improve the results to the quantum limit of sensitivity.

These measurements are preliminary. However, the measurement precision of $\sim$30 pm $\text{Hz}^{-1/2}$ has already exceeded the sensitivity ($\sim$1000 pm $\text{Hz}^{-1/2}$) of capacitive sensing by a factor of $\sim$30. The measurement distance of 1.5 cm is approximately four to eight times larger than that of the current capacitive sensing. At the power level of 1 mW, the back action force is estimated as 6.67×10^{-12} N using equation (2). For comparison, the back action force of a capacitive sensor using 1 V voltage, 1 cm^2 electrode and 2 mm gap produces a back action force of $\sim 2.8 \times 10^{-11}$ N, three times larger than that of the 1 mW laser. The optical sensing is thus easier to achieve balance in double-sided detection akin to capacitive sensing.

However, the capacitive sensing has the advantage of non-periodic reading of the displacement. Capacitive sensing is consistent with the electrostatic forcing in mechanical construction. Therefore future GRS sensing technology may well be a combination of optical and capacitive sensing with proper crossover design.

Our preliminary experiment demonstrates the key elements of the all-reflective grating-based, fibre-coupled interferometer that is an essential element of the proposed advanced GRS. The results clearly show that the grating-based optical readout offers advantages of improving the sensitivity and reducing the back action, and increasing the gap size simultaneously.

9. Conclusion

We have proposed a stand-alone GRS, in which the external laser beams do not interfere with the internal proof mass sensing for science referencing and for drag-free flight control. This results in higher measurement precision and the simplification of GRS structure.

Optical sensing within the GRS is complemented by capacitive sensing in that capacitive sensing can be used for initial proof mass positioning and for recapture on orbit if necessary. The optical sensing offers the possibility of a larger gap, the reduction of the capacitive forcing to zero, and higher sensitivity, lower back action and lower noise in operation. The use of reflective optics for interferometry and fibre optics for transport simplifies the optical configuration and avoids issues associated with transmissive optics, such as optical path length changes with temperature due to refractive index variations, and birefringence effects due to temperature variations and stress. The use of a double-sided grating in the housing wall of a GRS is a key element for relaying, with picometre precision, the measurement of the proof mass position across the wall to the reference surface on the outside of the GRS housing.

References

[1] LISA Science Team 2000 *System and Technology Report* ESA

[2] Heinzel G *et al* 2004 The LTP interferometer and phasemeter *Class. Quantum Grav.* **21** S581–7

[3] Buchman S *et al* 2004 The Stanford gravitational reference sensor *5th Int. LISA Symp. ESTEC (Noordwijk, The Netherlands, 12–6 July)*

[4] Phinney S 2003 The Big Bang Observer, BBO proposal

[5] Sun K-X, Allen G, Buchman S, DeBra D and Byer R L 2004 New thinking on gravitational and optical reference structure for LISA and BBO SLAC/KIPAC *Conf.: Beyond Einstein: From the Big Bang to Black Holes (Stanford Linear Accelerator Center, 12 May)*

[6] Sun K-X and Byer R L 1998 All-reflective Michelson, Sagnac, and Fabry–Perot interferometers based on grating beam splitters *Opt. Lett.* **23** 567

[7] Nguyen H T, Shore B W, Bryan S J, Britten J A, Boyd R D and Perry M D 1997 High-efficiency fused silica transmission gratings *Opt. Lett.* **22** 142

[8] Shore B W, Perry M D, Britten J A, Boyd R D, Feit M D, Nguyen T, Chow R and Li L 1997 Design of high-efficiency dielectric reflection gratings *J. Opt. Soc. Am.* A **14** 1124

[9] Schumaker B and Harb C 2003 LISA optical bench design propositions *Presentation (Sept.)*